

Geocarto International

ISSN: 1010-6049 (Print) 1752-0762 (Online) Journal homepage: www.tandfonline.com/journals/tgei20

Integration of sentinel optical and radar data in Google Earth Engine for mapping small complex agroforests of shade-grown coffee in northern Peru

Angel J. Medina , Rolando Salas López , Jhon A. Zabaleta-Santisteban , Katerin M. Tuesta-Trauco , Abner S. Rivera-Fernández , José A. Sánchez-Vega , Teodoro B. Silva-Melendez , Jhonsy O. Silva-López , Nilton B. Rojas Briceno , Marlen A. Grandez Alberca , Cecibel Portocarrero Díaz , Jaris Veneros , Manuel Oliva Cruz & Elgar Barboza

To cite this article: Angel J. Medina , Rolando Salas López , Jhon A. Zabaleta-Santisteban , Katerin M. Tuesta-Trauco , Abner S. Rivera-Fernández , José A. Sánchez-Vega , Teodoro B. Silva-Melendez , Jhonsy O. Silva-López , Nilton B. Rojas Briceno , Marlen A. Grandez Alberca , Cecibel Portocarrero Díaz , Jaris Veneros , Manuel Oliva Cruz & Elgar Barboza (2026) Integration of sentinel optical and radar data in Google Earth Engine for mapping small complex agroforests of shade-grown coffee in northern Peru, Geocarto International, 41:1, 2596243, DOI: 10.1080/10106049.2025.2596243

To link to this article: https://doi.org/10.1080/10106049.2025.2596243

© 2026 The Author(s). Published by Informa UK Limited, trading as Taylor & Francis Group.

Published online: 16 Feb 2026.

Submit your article to this journal

Article views: 1805

View related articles

View Crossmark data

Citing articles: 1 View citing articles

Full Terms & Conditions of access and use can be found at
https://www.tandfonline.com/action/journalInformation?journalCode=tgei20

GEOCARTO INTERNATIONAL
2026, VOL. 41, NO. 1, 2596243
https://doi.org/10.1080/10106049.2025.2596243

Taylor & Francis
Taylor & Francis Group

RESEARCH ARTICLE

OPEN ACCESS Check for updates

Integration of sentinel optical and radar data in Google Earth Engine for mapping small complex agroforests of shade-grown coffee in northern Peru

Angel J. Medina[a], Rolando Salas López[a], Jhon A. Zabaleta-Santisteban[a], Katerin M. Tuesta-Trauco[a], Abner S. Rivera-Fernández[a], José A. Sánchez-Vega[a], Teodoro B. Silva-Melendez[a], Jhonsy O. Silva-López[b], Nilton B. Rojas Briceno[c], Marlen A. Grandez Alberca[a], Cecibel Portocarrero Díaz[a], Jaris Veneros[a], Manuel Oliva Cruz[a] and Elgar Barboza[a]

[a]Instituto de Investigación para el Desarrollo Sustentable de Ceja de Selva (INDES-CES), Universidad Nacional Toribio Rodríguez de Mendoza de Amazonas, Chachapoyas, Perú; [b]Área de Cartografía y Teledetección, Laboratorio de Agrostología, Facultad de Ingeniería Zootecnista, Agronegocios, Biotecnología y Ciencia de Datos – FIZBAC, Universidad Nacional Toribio Rodríguez de Mendoza de Amazonas – UNTRM, Chachapoyas, Peru; [c]Grupo de Investigación en Ciencia de la Información Geoespacial – CIGEO, Instituto de Investigación para el Desarrollo del Perú, Universidad Nacional de Moquegua, Pacocha, Perú

ABSTRACT

Coffee is a key global export product; however, there is still limited information on the location and dynamics of its growing areas, especially in light of the implementation of new regulations such as the EUDR. This study used optical and radar data from the Sentinel satellite, processed on the Google Earth Engine (GEE) platform, to map vegetation cover and land use, including coffee farming systems in the province of Rodríguez de Mendoza. The Random Forest algorithm was applied, trained with 531 verification points collected in the field. As a result, six classified maps were generated, showing sustained growth in the area under coffee cultivation, from 7,111.071 ha to 9,443.050 ha over a six-year period. The cartographic products achieved high levels of accuracy, with Overall Accuracy (OA) values above 94% and a Kappa index (KI) above 88.9%. These results demonstrate the potential of GEE for multi-year monitoring of permanent.

ARTICLE HISTORY
Received 18 June 2025
Accepted 21 November 2025

KEYWORDS
Coffee; deforestation; random forest; remote sensing; SAR

1. Introduction

Coffee (*Coffea arabica*) is one of the most relevant agricultural crops globally, playing a strategic role in the economies of countries located within the equatorial belt between the Tropics of Cancer and Capricorn, known as the 'Bean Belt' (Nadaf et al. 2024). Its production significantly impacts forest cover, biodiversity, and human well-being (Hunt et al. 2020). In April 2024, global exports reached 11.96 million bags, surpassing the 10.24 million recorded in the same month of 2023 (ICO, 2024). Globally, the countries of Brazil, Vietnam, Colombia, Indonesia, Ethiopia, India, Honduras, Mexico, Peru, and Guatemala rank among the top coffee exporters, with Peru being among the top ten global coffee exporters in 2024 (FAOSTAT, 2024), which shows its economic importance for the country.

Given the strategic role of coffee in the global economy, it is essential to understand its influence on land use changes, particularly in relation to the loss or recovery of tropical forests (Hunt et al. 2020). According to the Food and Agriculture Organisation of the United Nations (FAO), in the last three decades, the planet has lost approximately 420 million hectares of forest cover—a phenomenon that primarily affects tropical and subtropical regions, where agricultural expansion accounts for nearly 90% of this deforestation (viviennehalleux and europarleuropaeu, 2022). In Peru, nearly 3 million hectares of Amazonian forests were lost between 2001 and 2022 (Rojas-Briceño et al. 2025).

In response to this environmental issue, the European Union Regulation on Deforestation-Free Products (EUDR) came into force on June 29, 2023. This regulation requires that operators and traders

CONTACT Manuel Oliva Cruz manuel.oliva@untrm.edu.pe

© 2026 The Author(s). Published by Informa UK Limited, trading as Taylor & Francis Group.
This is an Open Access article distributed under the terms of the Creative Commons Attribution-NonCommercial License (http://creativecommons.org/licenses/by-nc/4.0/), which permits unrestricted non-commercial use, distribution, and reproduction in any medium, provided the original work is properly cited. The terms on which this article has been published allow the posting of the Accepted Manuscript in a repository by the author(s) or with their consent.

who place or export certain commodities (such as meat, timber, cocoa, soy, palm oil, coffee, rubber, and their derivatives) ensure they are traceable and originate from areas that are not recently deforested or affected by forest degradation (European Commission, 2024).

To respond to these regulatory requirements, it is essential to develop detailed geospatial maps of the different coffee production systems, which allow for effective monitoring of the loss or regeneration of tropical and native forests. However, the generation of geospatial information on these crops is often limited due to the diversity and complexity of coffee-growing systems. Additionally, one of the main challenges in the remote detection of coffee is the persistent cloud cover present in the tropical 'coffee belt' (Fangjie et al. 2023; Li et al. 2021; Maskell et al. 2021a). In the face of this challenge, remote sensing has emerged in recent years as an efficient and accessible tool for generating reproducible and low-cost information on land use and land cover (LULC) (Hunt et al. 2020).

Recent studies have demonstrated the potential of advanced classification algorithms, along with high-resolution airborne and satellite passive data, to improve the discrimination of agroforestry systems managed by both small and large producers (dela Torre et al. 2021; Sarzynski et al. 2020; Vilela et al. 2024; Vincent M and Varalakshmi 2024). However, despite previous studies, the literature still presents significant gaps, as there is no single mapping model that identifies and relates the most relevant spectral indices and determines, among different machine learning algorithms, the most efficient for this purpose (Condro et al. 2020; Vilela et al. 2024). Therefore, accurately detecting shade-grown coffee using satellite imagery has remained a constant challenge due to spectral similarity with secondary forest cover and young jungles, resulting in classification errors and limiting the understanding of productive systems in mixed landscapes (Kelley et al. 2018).

The exponential growth in the use of Big Data, open access to high-resolution satellite imagery, and the development of cloud-based analysis platforms such as Google Earth Engine (GEE) have significantly enhanced geospatial analysis capabilities in agriculture, mainly through the use of improved algorithms for crop mapping (Adrian et al. 2021). GEE allows the integration of large volumes of multitemporal and multispectral information with machine learning algorithms, facilitating efficient, reproducible, and scalable crop classification (Zhi et al. 2022). Unlike optical images, Synthetic Aperture Radar (SAR) imagery is sensitive to changes in growth stages and morphological structures, providing complementary information on vegetation canopy structure, surface roughness, and moisture content (Cui et al. 2020; Moraiti et al. 2024). In South America, several studies have implemented combined approaches using optical and radar sensors to identify agroforestry systems. For instance, in Colombia Bolívar and Reu (2021), roposed using field measurements of vegetation structure along with Sentinel–2 imagery to remotely detect agroforestry systems by employing spectral and textural variables and exploring the potential for biodiversity preservation in tropical agriculture. Similar research has been carried out in Brazil (Ferreira et al. 2024), México (Escobar-López et al. 2024) and Peru (Barboza et al. 2024; Gómez-Fernández et al. 2024) demonstrating the regional applicability of these methodologies.

On the other hand, the effectiveness of semi-automatic approaches using the Random Forest (RF) algorithm and the fusion of optical and radar imagery has been widely recognised in land cover classification within agroforestry plantations (Sarzynski et al. 2020). The RF algorithm, as a non-parametric classifier, is one of the most widely used in remote sensing due to its ability to handle large volumes of data, avoid overfitting, and provide high-accuracy results (van Beijma et al. 2014). In this regard, the fusion of multi-source data such as Sentinel, PlanetScope, and SAR has shown superior performance, with overall classification accuracies close to 84% and producer and user accuracy levels reaching up to 84% and 90%, respectively (Liu et al. 2023). The findings indicate that integrating optical data (Sentinel–2 and PlanetScope) and SAR (Sentinel–1) in GEE significantly outperforms the use of individual sources, being key both in the classification stage and in data preprocessing (Adrian et al. 2021).

In this study, a methodology was developed based on the integration of optical imagery (Sentinel–2) and radar imagery (SAR; Sentinel–1) on the GEE platform, with the aim of identifying and assessing land use changes associated with forest conversion into coffee production systems, in compliance with the new EUDR regulation. This was due to the lack of updated and accurate information on cultivation areas, productivity, and the sustainability of coffee in Peru. The research focused on the province of Rodríguez de

Mendoza (Amazonas, Peru), where four types of coffee farming systems were characterised: traditional polyculture, commercial polyculture, monoculture with shade, and monoculture without shade. Classification was carried out using the RF algorithm and validated using standard accuracy metrics. Therefore, the purpose of the study was to generate accurate and replicable geospatial information that contributes to improving production traceability, territorial management, and compliance with international environmental standards.

2. Materials and methods

2.1. Study area

The province of Rodríguez de Mendoza, located in the southeast of the Amazonas department (Peru), is one of the main coffee-growing areas in the country, with more than two decades as its primary economic driver (L. García et al. 2024). Its territorial extension is approximately 258,233.079 ha (Figure 1), and it is composed of 12 districts that are home to a population of around 32,130 inhabitants (INEI, 2017). The predominant climate is warm and humid (Campos Baca et al. 2019), characterised by geography with a marked altitudinal variation between 700 and 3900 metres above sea level. For this study, the analysis area was limited to zones with agroecological potential for coffee cultivation, ranging between 700 and 2800 metres above sea level, according to the optimal ranges defined using a Digital Elevation Model (DEM) (Escobar-López et al. 2022; Salas et al. 2020).

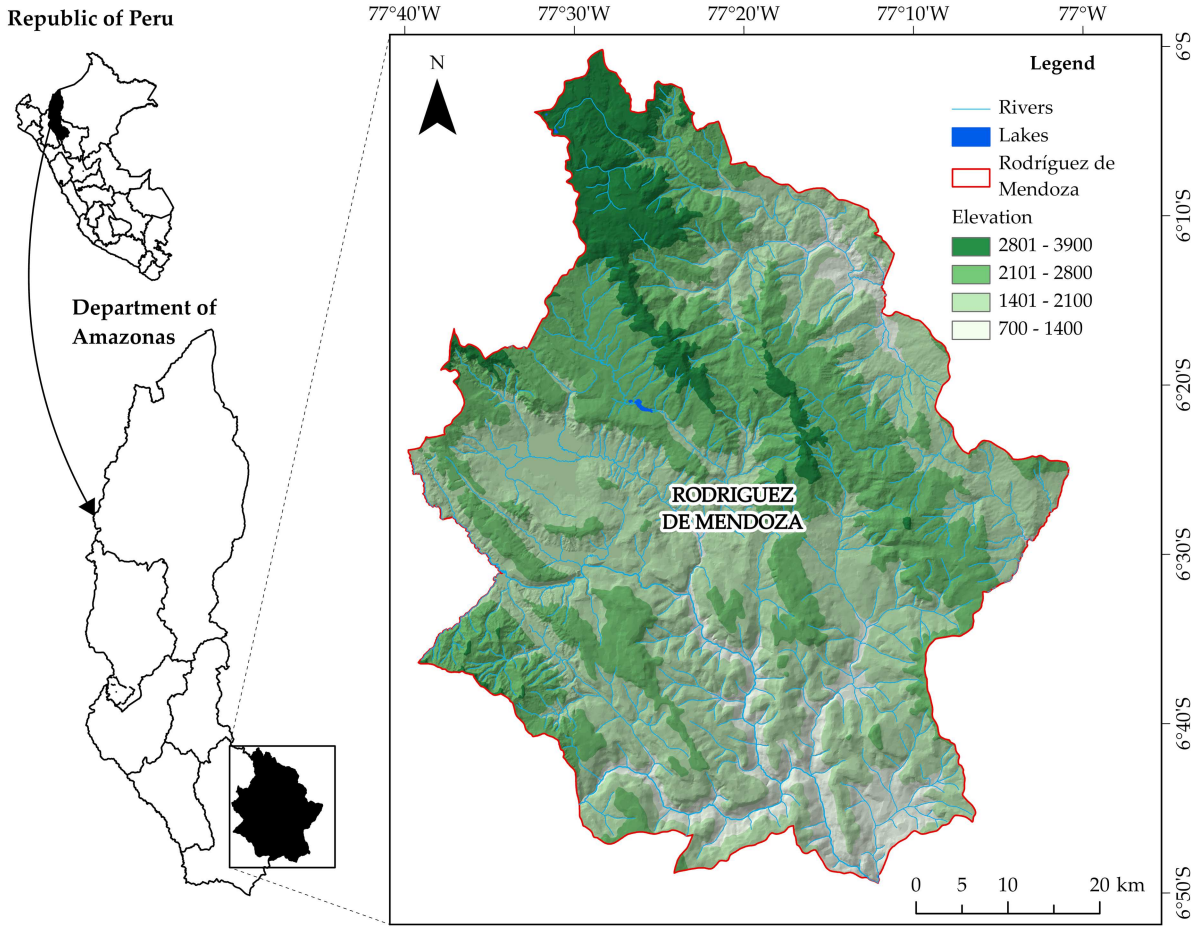


Figure 1. Location of the study area: Province of Rodriguez de Mendoza in the department of Amazonas.

2.2. Methodological procedure

Figure 2 illustrates the methodological diagram used to map coffee production systems using imagery from the Sentinel–1 and Sentinel–2 missions, processed on the GEE platform during the study period 2019–2024 (Yang et al. 2022). The workflow was organised into three main parts: Preprocessing, Classification, and Mapping. In the preprocessing phase, began with the spatial preparation of the study area, followed by the input of Optical and SAR images, the application of filters and parameter settings, as well as the calculation of spectral indices and topographic variables (loading an SRTMGL1 DEM and generating elevation, slope, aspect, and hillshade maps).

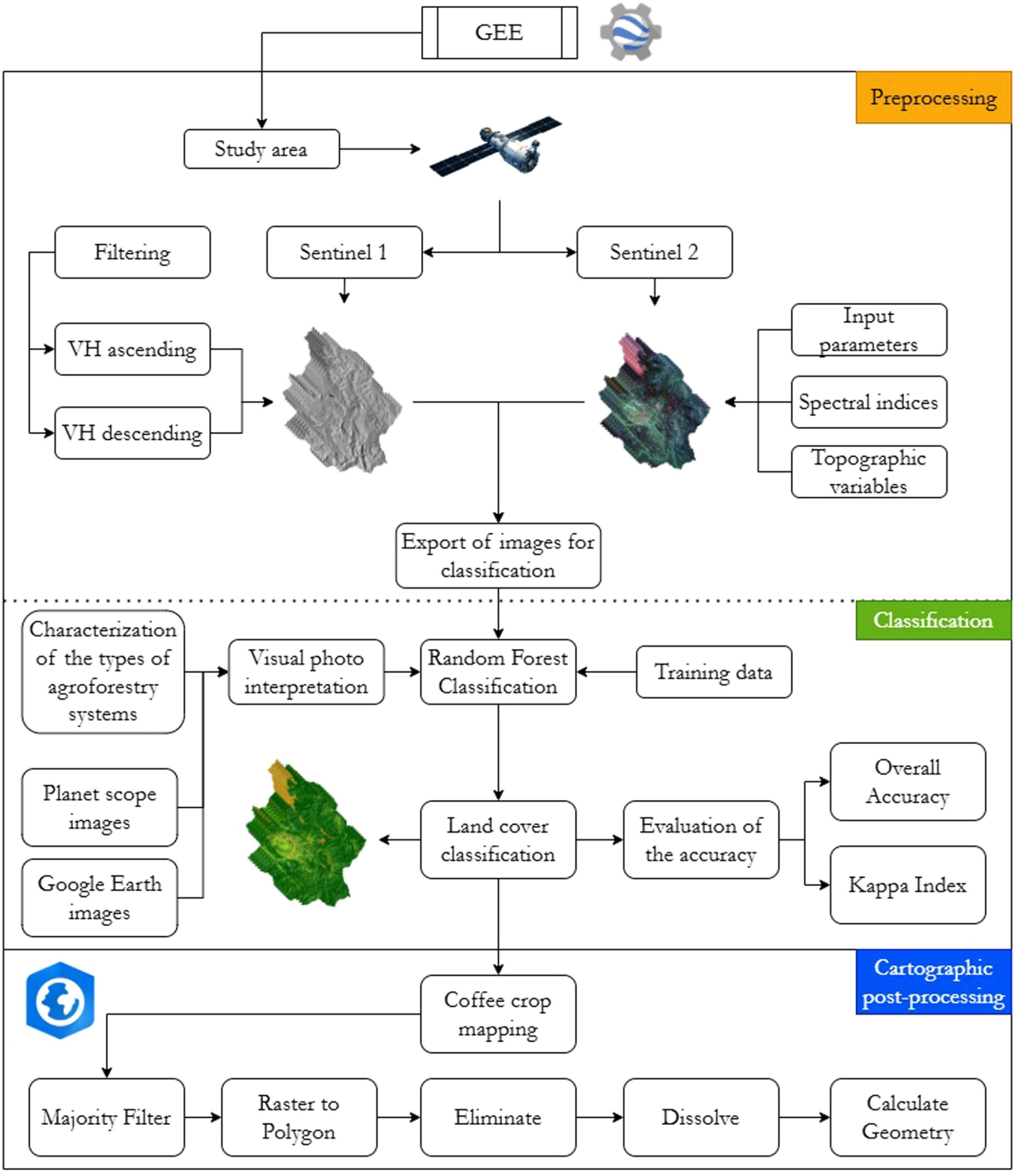


Figure 2. Methodological Flowchart for mapping shade-grown coffee crops.

The classification was carried out on the same platform using the RF classifier, based on the results of image preprocessing for all years to be evaluated. To this end, 531 training and validation points collected in the field were incorporated, complemented by the visual interpretation of high-resolution images from PlanetScope and Google Earth. Finally, the classified maps underwent a cartographic postprocessing stage, in which spatial filters were applied to reduce 'salt and pepper' noise using ArcGIS Pro software (version 3.0.1), with tools such as Majority Filter, Eliminate, and Dissolve.

2.3. Characterisation of coffee production systems

For the characterisation of coffee production systems, technical-productive information was collected from local associations, cooperatives, and agricultural organisations, complemented by field data from each district within the study area (Escobar-López et al. 2022), The collected data included: type of coffee planted, geographic coordinates of the centre of each plot, number of plantations, coffee varieties, botanical species used as shade, planting density, and reference photographs (Grandez-Alberca et al. 2025).

A total of 531 training points were collected, distributed as follows: 54 from 2019, 34 from 2020, 84 from 2021, 97 from 2022, 114 from 2023, and 148 from 2024. In addition, the points corresponding to the last year (2024) were classified into four types of production systems: traditional polyculture (60.1%), commercial polyculture (20.3%), monoculture with shade (16.9%), and monoculture without shade (2.7%), similar to the study by Hunt et al. (2020). These systems were defined according to agroecological criteria established by Moguel and Toledo (1999), as shown in Figure 3.

2.4. Image preprocessing

Various studies have evaluated land cover dynamics at multiple spatial scales in order to monitor crops by leveraging the capabilities of the GEE platform (Htitiou et al. 2021). It provides access to a vast collection of satellite imagery and advanced analytical tools for managing geospatial big data, enabling agile and scalable analysis processes thanks to Google's cloud computing infrastructure (Becker et al. 2021). In the specific mapping of crop plantations, both the research community and operators often use spatial information. Cloud-based platforms like GEE facilitate access to medium- and high-resolution satellite data, such as imagery from the Multi Spectral Instrument (MSI) sensors of Sentinel–2, Thematic Mapper (TM) and Enhanced Thematic Mapper (ETM+), Operational Land Imager, and Thermal Infra-red Sensor (OLI.TIRS) (Onojeghuo et al. 2023). The efficiency of the GEE platform stands out in executing complex workflows, such as the fusion of multitemporal data and the generation of spectral indices, making it a key tool for large-scale agricultural mapping projects (Shelestov et al. 2017).

2.4.1. Data set

During the preprocessing stage, two products were generated for each year:

- The Digital Elevation Model (DEM) used in this study to generate the topographic variables corresponds to the SRTMGL1 v003 product of the Shuttle Radar Topography Mission, developed by NASA and the USGS. This model, available in Google Earth Engine, provides a spatial resolution of 30 metres (1 arc-second) and near-global coverage between latitudes 60°N and 56°S (Farr et al. 2007).
- Sentinel–2 satellite imagery, which offers a high revisit frequency of 5 days at the Equator, thanks to its MultiSpectral Instrument (MSI), in the Harmonised Sentinel–2 MSI: Level-2A SR version (Wyss, 2015). This sensor provides 13 spectral bands, from which seven specific bands were selected 'B2', 'B3', 'B4', 'B5', 'B8', 'B11', 'B12' (with 10-metre resolution: 'B2', 'B3', 'B4', 'B8' and 20-metre resolution: 'B5', 'B11', 'B12'), corresponding to the 'blue', 'green', 'red', 're1', 'nir', 'swir1', and 'swir2' bands (Harmonised Sentinel–2 MSI: MultiSpectral Instrument, Level-2A (SR) | Earth Engine Data Catalogue | Google for Developers, n.d.).

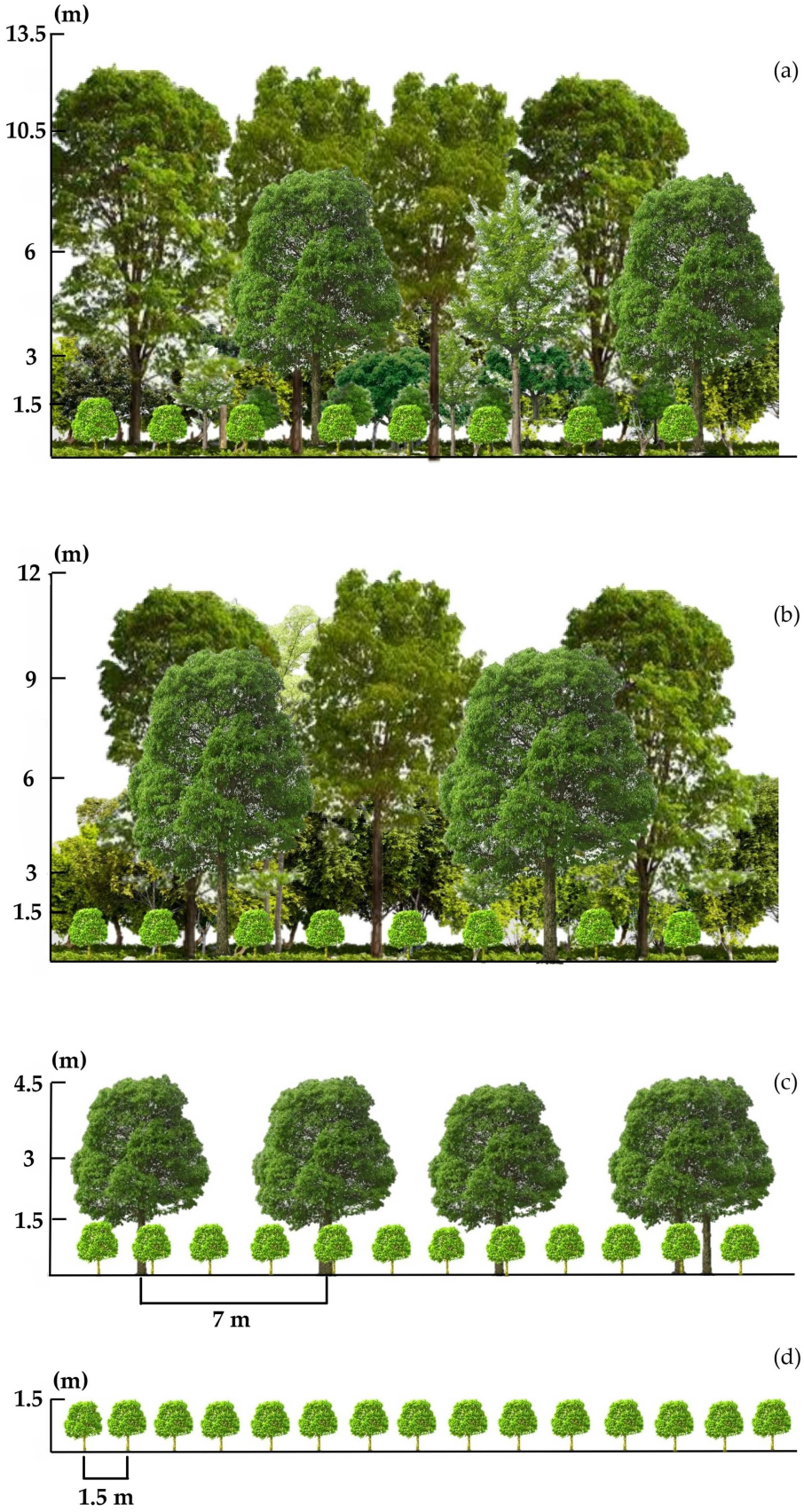


Figure 3. Classification of coffee planting systems, (a) Traditional polyculture, (b) Commercial polyculture, (c) Monoculture with shade, (d) Monoculture without shade.

The images used have a spatial resolution of 10 and 20 metres and were continuously collected from January 1 to December 31 of each year.

- Sentinel−1 satellite imagery, which collects C-band Synthetic Aperture Radar (SAR) images in Ground Range Detected (GDR) format (Google Earth Engine, 2025), This sensor provides data with a temporal resolution of 12 days, allowing for various polarisation combinations. In this study, both combinations were used: ascending VH and descending VH, captured during the same annual period (January to December).

2.4.2. Incorporation of auxiliary variables

To improve the quality of the information derived from satellite imagery, auxiliary spectral variables derived from the reflectance of different bands were incorporated. These indicators are essential for the classification of agroforestry cover, vegetation zones, and forest ecosystems (Vincent M and Varalakshmi 2024), as they highlight biophysical properties such as chlorophyll content, soil moisture, or the presence of surface water. In this study, various vegetation, soil, and water indices applicable to Sentinel−2 were calculated to enhance supervised classification, as shown in Table 1.

2.4.3. Image grouping and filtering

All available images from the Sentinel−1 and Sentinel−2 missions were used with the objective of generating a detailed land cover map of the coffee-growing landscape, identifying eight distinct classes (Maskell et al. 2021b), These images were grouped and filtered according to the temporal ranges corresponding to each year of analysis, applying atmospheric corrections and filters to reduce cloud presence (Aji et al. 2023; Pahlevan et al. 2021). The results were evaluated on a multi-year basis, covering the period evaluated in this research.

2.4.4. Export of generated maps

To optimise the management of computational resources in GEE, the processed images (10 m/pixel and Coordinate Reference System EPSG:3857) during the preprocessing stage were exported as intermediate files (annual mosaics and spectral composites) to the platform's internal storage system. This strategy allowed the retention of intermediate results and ensured workflow continuity. Subsequently, these files were used as inputs in a new script developed for the land cover classification stage, thereby optimising the use of computational resources and facilitating efficient integration of the processed data.

Table 1. Vegetation, soil and water indices.

Index	Description	Formula	References
NDVI	Normalised Different Vegetation Index	$NDVI = \left(\frac{nir - red}{nir + red}\right)$	Rouse et al. (1973)
MSAVI	Modified Soil Adjusted Vegetation Index	$MSAVI = \frac{2 * nir + 1v((2 * nir)\hat{}2 - 8 * (nir - red))}{2}$	Qi et al. (1994)
EVI	Enhanced Vegetation Index	$EVI = 2.5 * \frac{nir - \text{red}}{nir + (6 * red) - (7.5 * blue) + 1}$	Huete et al. (2002)
GCVI	Green Chlorophyll Vegetation Index	$GCVI = (nir/green)$ -1	Gitelson et al. (2003)
NDWI	Normalised Difference Water Index	$NDWI = \left(\frac{swir1 - nir}{swir1 + nir}\right)$	Gao (1996)
MNDWI	Modified Normalised Difference Water Index	$MNDWI = \frac{\rho green - \rho swir}{\rho green + \rho swir}$	Xu (2006)
MODCRC	Modified Crop Residue Cover	$MODCRC = \left(\frac{swir1 - green}{swir1 + green}\right)$	Hobbs et al. (2007)
NDTI	Normalised Difference Tillage Index	$NDTI = \left(\frac{swir1 - swir2}{swir1 + swir2}\right)$	Van Deventer et al. (1997)
NBRI	Normalised Burn Ratio Index	$NBRI = \left(\frac{nir - swir2}{nir + swir2}\right)$	M. J. L. García and Caselles (1991)
TVI	Transformed Vegetation Index	$TVI = 60 * (nir — green) — 100 * (nir — green)$	Thenkabail et al. (2000)
MTCI	MERIS Terrestrial Chlorophyll Index	$MTCI = \left(\frac{nir - re1}{nir + re1}\right)$	Dash and Curran (2004)
STI	Simple Tillage Index	$STI = \left(\frac{swir1}{swir2}\right)$	Van Deventer et al. (1997)
ARVI	Atmospherically Resistant Vegetation Index	$ARVI = \left(\frac{nir - RB}{nir + RB}\right)$	Houghton et al. (2001)
		$RB = red — C * (blue — red)$, $C = 1$	

2.5. Classification

2.5.1. Training and validation data

The study was based on a balanced sample of 531 training points for the main land cover evaluated in this research, obtained through GPS records and georeferenced photographic documentation (Atalaya-Marin et al. 2025) (Figure 4), which were highly useful for the development of the machine learning algorithm (Gumma et al. 2022). This information was collected directly on-site (from October 7 to 11, 2024; and from November 25 to 29, 2024) and thanks to data provided by the Alta Montaña cooperative of the Rodríguez de Mendoza province. A balanced sample was used given our emphasis on achieving not only high accuracy in mapping shade-grown coffee but also high overall classification accuracy (Kelley et al. 2018). In our case, it was not possible to completely randomise the training data collection due to time constraints in the field and the participatory nature of the research project.

2.5.2. Classification with random forest

The supervised classification was developed in GEE for each year analysed. Although GEE offers multiple classification algorithms—including maximum entropy, support vector machines (SVM) with linear, polynomial, and Gaussian kernels, classification trees, and naive Bayes classifiers (Single-Page API Reference | Google Earth Engine | Google for Developers, n.d.), in this study, RF was used with *ntree* = *300* to ensure prediction stability without significantly increasing computational cost. The *mtry* parameter was set to its default value, determined as the square root of the total number of predictor variables, following the standard recommendation for multivariable classification problems. This classifier was chosen due to its robustness, computational efficiency, and proven performance in multiclass classification tasks with heterogeneous satellite data (Ouma et al. 2022).

Satellite images are classified and pixels showing the greatest similarity within the same class are detected (Vincent M and Varalakshmi 2024). However, before classification, training samples (polygons or points collected in the field) were used to generate the annual maps, located in different areas representing the various types of coffee cultivation systems. For the purposes of this research, they were grouped into eight major classes. Therefore, the study area was classified as coffee without shade and with shade, forest, herbaceous or shrubland, urban, water, bare soil, pasture, and Montane Grasslands and Relicts (MGR).

The RF algorithm was configured to perform pixel-based classification, using both the selected spectral bands and the derived indices and auxiliary variables (Zeng et al. 2022). This method is widely recognised for its high accuracy in generating land use and land cover (LULC) maps from multispectral images (Gómez Fernández et al. 2022; Ouma et al. 2022). To train the model, 531 georeferenced points were used, along with variables from the most suitable dataset (Vilela et al. 2023). This enabled the generation of LULC maps with a spatial resolution of 10 metres, consistent with Sentinel–2 imagery. Finally, a

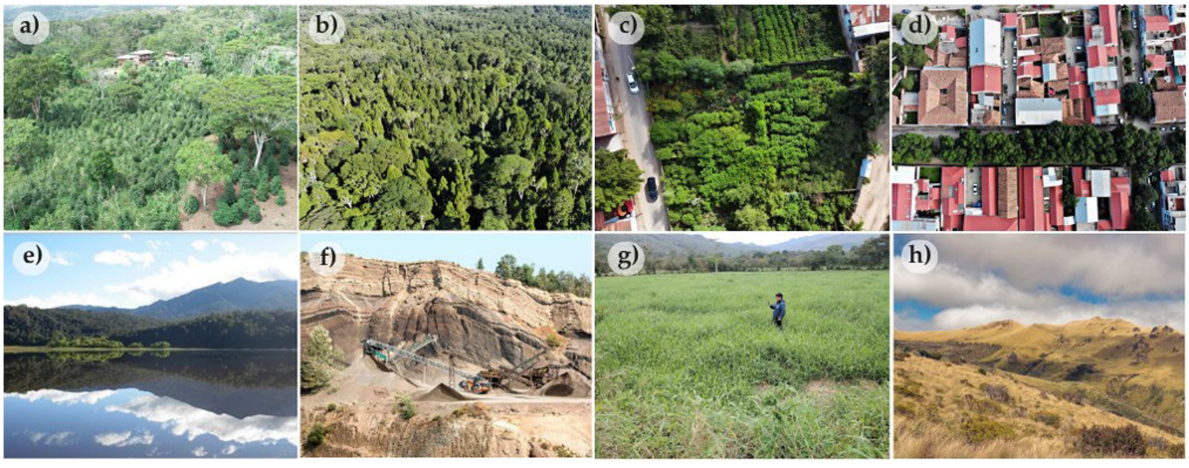


Figure 4. Visual representation of the land cover classes used in the supervised classification: a) Coffee, b) Forest, c) Herbaseus, d) Urban, e) Water, f) Bare soil, g) Pasture and h) Montane grasslands and relicts.

post-classification process and visual review were applied to improve the final quality of the generated products (Breiman 2001).

2.5.3. Accuracy assessment

The accuracy of all RF models developed was evaluated through various quantitative and qualitative approaches. First, confusion matrices were used, which compare the classifier's predictions with reference data validated in the field and through visual interpretation, thus facilitating an objective assessment of the model's performance.

In addition, a visual assessment of spatial consistency was carried out, comparing the land cover maps generated with freely available products such as Google Earth Pro and high-resolution images from PlanetScope, which allow the percentage of tree canopy cover to be estimated. This information, with a spatial resolution of 10 metres, was useful for visually verifying the spatial coherence of the classified map.

To quantify the overall accuracy of the results and provide a statistical measure of the algorithm's performance, two widely used indicators in LULC classification studies were calculated: Overall Accuracy (OA) and Kappa Index (KI) (Wang et al. 2023). These indicators allow for interpreting the model's reliability, considering ranges from unacceptable results (values below 0.5) to acceptable and robust levels of accuracy (values above 0.90) (Landis and Koch 1977).

2.6. Map generation in ArcGIS pro

The products generated in GEE were exported to ArcGIS Pro software (version 3.1.5) for the purpose of optimising the cartographic quality of the obtained maps. A spatial filter was applied to reduce the 'salt and pepper' effect. In addition, a precise calculation of the areas corresponding to each evaluated land cover class was performed (Medina-Medina et al. 2024). This process included the use of various geoprocessing tools available in the ArcGIS Pro toolbox, such as Majority Filter, Raster to Polygon, Eliminate, Dissolve, and Calculate Geometry. Finally, the preparation and presentation of the maps were carried out within the same platform, ensuring a clear, professional, and easily interpretable cartographic representation.

3. Results

3.1. Distribution and availability of data

Table 2 details the availability of satellite images used in the analysis for the period 2019–2024. In the case of Sentinel–1, interannual variations were observed in the number of available scenes for both Descending Vertical–Horizontal polarisation (VHD) and Ascending Vertical–Horizontal polarisation (VHA). The year 2023 recorded the highest number of images in both polarisations, with 86 VHD scenes and 108 VHA scenes, which contributed to greater accuracy in land cover classification. In contrast, the lowest number of images was recorded in 2021, with only 53 VHD scenes and 57 VHA scenes.

On the other hand, the optical data from Sentinel–2 showed high availability throughout the entire study period, with an average of approximately 285 images per year. The highest number of scenes was obtained in 2019 (293 images), while 2024 showed a slight decrease, with 264 available scenes, due to the date range being limited from January to October of that year. This high availability of multitemporal data allowed for adequate coverage of the study area and supported a detailed analysis of land use changes.

Table 2. Data availability for S1 and S2.

	Sentinel-1		
Year	VHD	VHA	Sentinel-2
2019	61	42	293
2020	59	61	291
2021	53	57	292
2022	64	102	294
2023	86	108	280
2024	77	94	264

Table 3. Accuracy metrics for each evaluated year.

Year	OA	KI
2019	96.70%	0.948
2020	96.10%	0.926
2021	96.60%	0.952
2022	97.00%	0.956
2023	94.80%	0.889
2024	96.30%	0.948

3.2. Precision metrics

The accuracy metrics obtained during the land cover classification process demonstrate a highly satisfactory performance of the model (Table 3). Overall Accuracy (OA) remained above 94.0% in all evaluated years, reaching its highest value in 2022 (97.0%), followed by 2019 and 2021 (with 96.7% and 96.6%, respectively). Likewise, the Kappa Index (KI), which accounts for agreement beyond chance, confirmed the robustness of the classification, with values exceeding 0.92 in most cases. The highest KI value was also recorded in 2022 (KI = 0.956), indicating an excellent level of agreement. Although a slight decrease was observed in both metrics in 2023 (OA = 94.8%, KI = 0.889), the overall performance of the model remained within acceptable and reliable ranges for multitemporal LULC analysis.

On the other hand, the performance of the classification model was evaluated using annual confusion matrices for the period 2019–2024. Overall, a high level of classification accuracy was observed across classes, with the 'Coffee' class standing out for its user accuracy, which exceeded 83% in all years, reaching its highest value in 2024 (93.2%). The 'Forest' and 'Herbaceous' classes also showed consistent results, with values close to or above 95%. Meanwhile, 'Urban' and 'Water' classes exhibited clear spectral separation, reflected in accuracy levels above 94%. However, slight misclassifications were identified between classes with similar spectral characteristics, such as 'Herbaceous' and 'Pasture,' particularly in 2020 and 2021. Nevertheless, these confusions did not significantly compromise the overall robustness of the model, which demonstrated stable and reliable performance throughout the analysed period (Figure 5).

3.3. 2019–2024 land cover classification

Figure 6 presents the land cover classification results for the coffee-growing landscape during the 2019–2024 period. Eight thematic classes were identified: coffee, forest, shrub and herbaceous vegetation, urban, water, bare soil, pasture, and montane grasslands and relicts (MGR). This time series reveals relevant spatial change patterns such as the expansion or contraction of coffee cultivation, forest fragmentation, and transitions between productive systems and natural areas. These maps provide a fundamental basis for the multi-annual analysis of land use and land cover changes within the study area.

3.4. Detailed land cover mapping by 2020

As part of the analysis, a land cover classification map for the year 2020 was developed (Figure 7). This result is a key element for verifying compliance with the EUDR, which establishes that products such as coffee, cocoa, soy, beef, palm oil, wood, rubber, and their derivatives must not originate from land that has been deforested after December 31, 2020. Therefore, this map can be used to identify areas with forest cover prior to that date and serves as a baseline for detecting potential land use changes associated with deforestation.

3.5. Distribution of areas for each class

Figure 8 shows the distribution of the area occupied by each land cover class in the coffee landscape during the period 2019–2024. The 'Forest' class consistently represents the largest area throughout all evaluated years, although it shows a slight decreasing trend, which may indicate a progressive loss of forest cover. In contrast, the 'Herbaceous', 'Pasture', and 'Coffee' classes exhibit more evident interannual variability, highlighting a gradual increase in coffee cultivation, possibly associated with agricultural expansion.

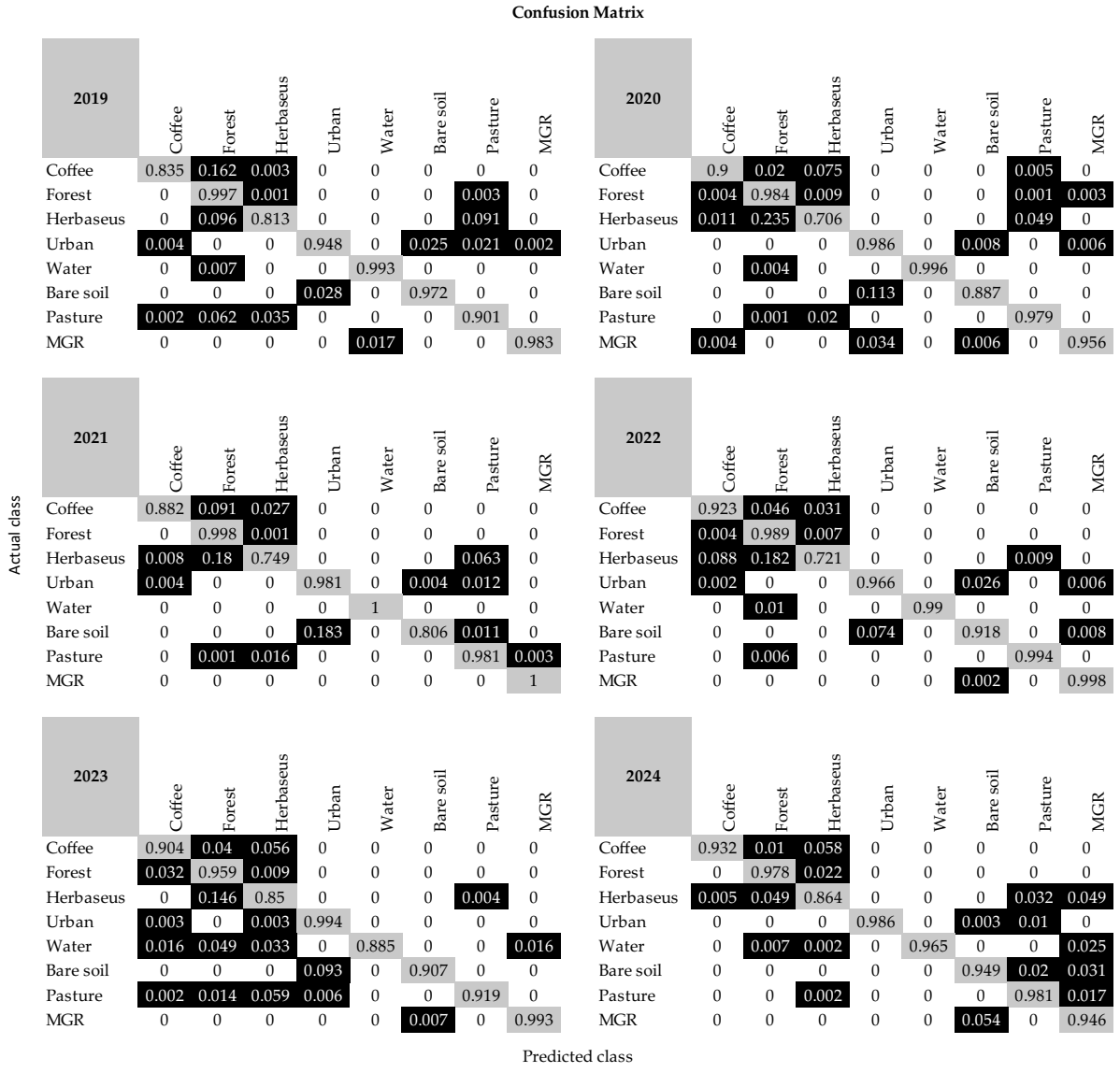


Figure 5. Confusion matrices for each classified year (2019–2024).

Meanwhile, the 'Urban', 'Bare soil', and 'Water' categories occupy very small portions of the territory, remaining practically constant.

On the other hand, the previous figure shows that the coffee land cover class experienced a steady increase between 2019 and 2024. In 2019, the classified area was 7,111.071 hectares, progressively increasing to reach 9,443.050 hectares in 2024. This growth represents a total increase of approximately 32.75% over six years. The largest year-over-year increase occurred between 2021 and 2022, when the cultivated area rose from 7,415.185 ha to 8,876.205 ha, reflecting a significant expansion of coffee cultivation.

3.6. Spatial mapping of coffee coverage for 2019–2024

A set of thematic maps was generated to exclusively represent the spatial distribution of coffee cultivation in the study area during the 2019–2024 period (Figure 9). This spatial visualisation allows for a clearer observation of the crop's expansion across the territory, highlighting a progressive increase in its coverage in various areas, especially on hillsides and mid-mountain zones, between 900 and 2500 metres above sea level. This detailed visualisation enables the identification of hotspots of significant cultivation growth,

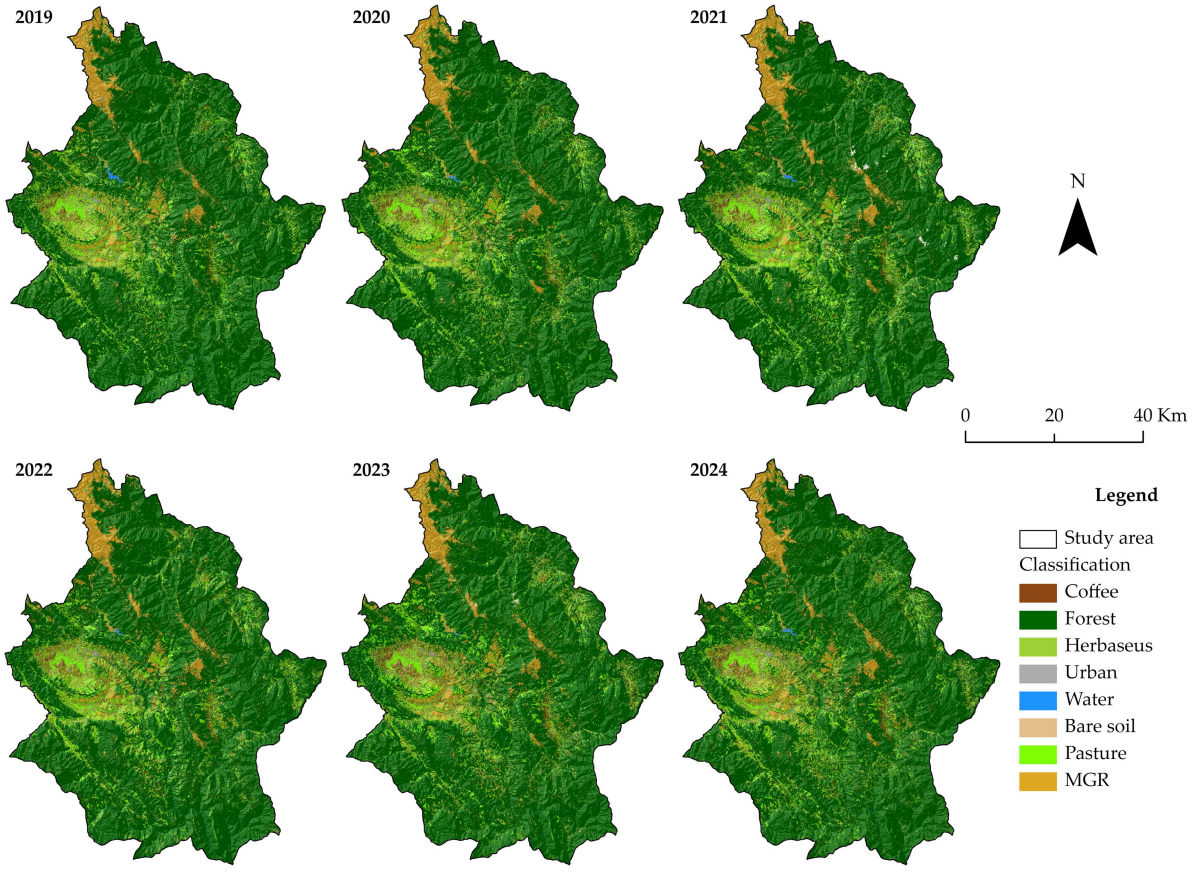


Figure 6. Annual land cover classification series in Rodríguez de Mendoza (2019–2024).

which may be associated with both favourable agroecological factors and land-use decisions made by local producers. The temporal comparison reveals a continuous upward trend, consistent with the results obtained from the supervised classification.

4. Discussion

The mapping of complex shaded coffee landscapes represents a fundamental step in understanding land use and land cover change dynamics in coffee-producing departments and provinces. This research developed a province-scale methodology focused exclusively on permanent crops such as coffee, in contrast to previous studies that prioritised annual crops like rice, maize, soy, or banana (dela Torre et al. 2021; Gumma et al. 2022; Medina-Medina et al. 2024; Vincent M and Varalakshmi 2024). The adopted approach integrates open-access satellite imagery (Sentinel, PlanetScope, and Google Earth Pro) and advanced geospatial classification techniques, aligned with recent efforts to map permanent production systems, such as those by Maskell et al. (2021), taking into account various coffee production classes and responding to new regulatory demands such as the EUDR.

Google Earth Engine (GEE) was employed as the central platform for data processing and classification due to its capabilities in handling large volumes of satellite data, as well as its robustness, operational efficiency, and open access. This choice also supports the replicability and scalability of the approach across different geographic and temporal contexts (Yang et al. 2022). Furthermore, its native integration with sensors such as Sentinel and compatibility with advanced classification algorithms like Random Forest make it an ideal platform for complex geospatial research. This versatility has led to its adoption in numerous recent studies, such as Moraiti et al. (2024), who evaluated the classification of cacao production systems; Barboza et al. (2024) who analysed the spatial and temporal dynamics of burned areas; and Gómez-Fernández et al. (2024), who studied historical change and landscape fragmentation using GEE.



Figure 7. Classified land cover for the year 2020 in Rodríguez de Mendoza, identifying eight land use types using Random Forest in Google Earth Engine.

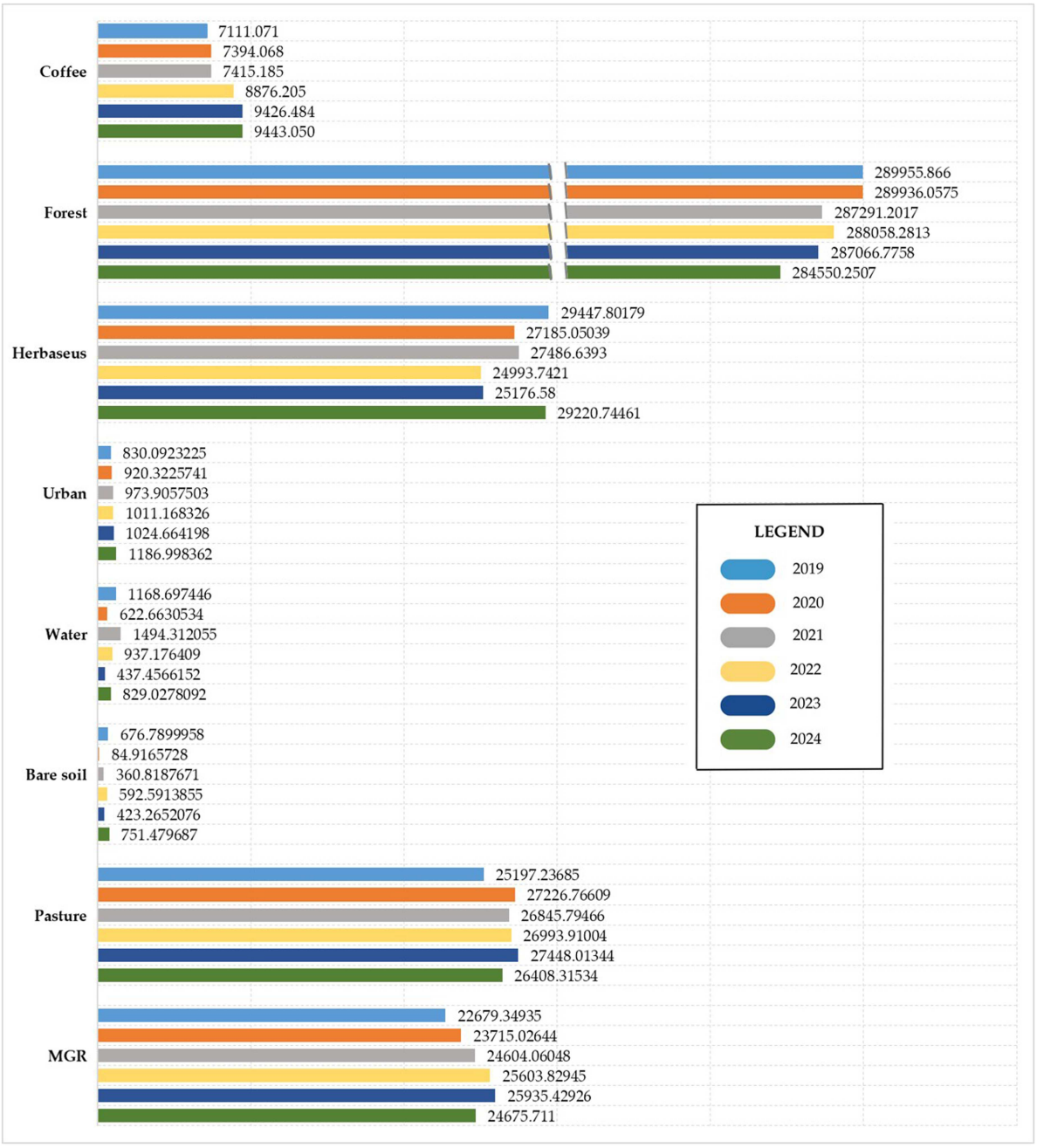


Figure 8. Distribution of areas for each land cover class.

The RF classifier was used within the GEE platform due to its high accuracy. This algorithm is widely recognised for its effectiveness in land cover classification, as it combines multiple decision trees to improve result accuracy and reduce overfitting. Its integration in GEE enables efficient and scalable application in agricultural monitoring studies such as coffee cultivation. This aligns with Vilela et al. (2024), whose research confirms that the best model for estimating infestation was the RF classifier, with an initial study yielding user and producer accuracy above 80%. Similarly, in a second study, they reported results with an accuracy of 0.86, a kappa index of 0.64, and a precision of 0.87.

In this research, the classification achieved consistent values of overall accuracy (OA > 94%) and Kappa index (KI > 0.92), confirming the reliability of the results. Similarly, Maskell et al. (2021a) reported an initial effort to distinguish at large scale different production styles within the same crop, which has important implications for various applications. In their study, they obtained a binary map with an overall

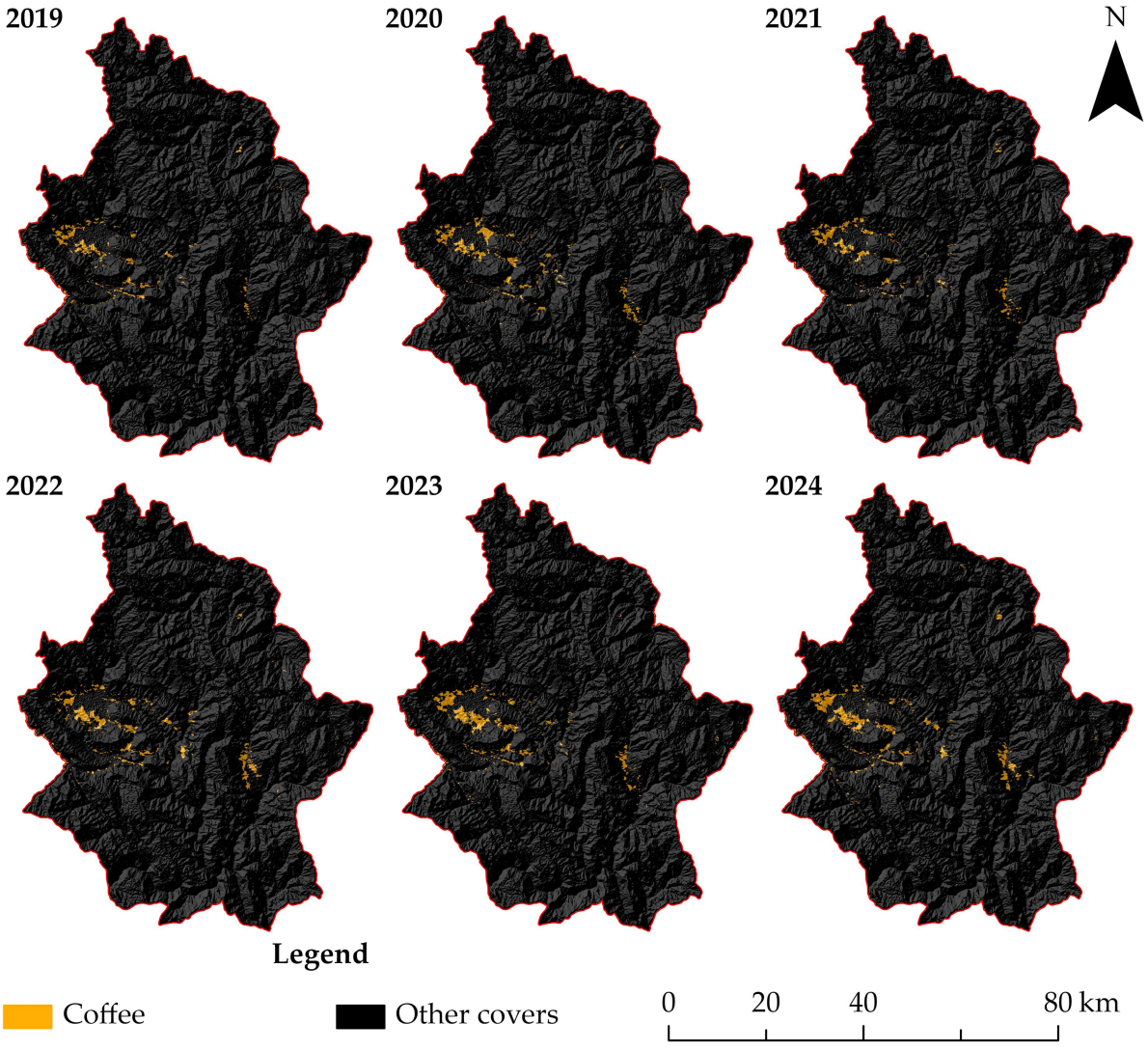


Figure 9. Spatial mapping of coffee crops in the province of Rodriguez de Mendoza.

accuracy of 89%, as well as user accuracies of 65%, 56%, and 71% for sun-grown coffee, intercropped coffee, and newly planted coffee, respectively. Along the same lines, studies conducted on similar crops also reported acceptable accuracy levels. Likewise, Atalaya-Marin et al. (2025), mapped a total of 4,338.6 ha of cacao monocultures and agroforestry systems, achieving an OA of 85% and a KI of 0.81.

On the other hand, large-scale agricultural mapping entails a series of technical challenges, among which the management of enormous volumes of satellite data and the demand for advanced computational capabilities stand out (Htitiou et al. 2021). One of the most critical challenges identified in this type of study is the availability and quality of training data, which are essential to ensure accurate classification. In this research, this limitation was overcome through the systematic collection of 531 georeferenced points corresponding to the main land cover class (coffee cultivation), which allowed for high levels of classification accuracy. These results contrast with those reported by Condro et al. (2020), who documented an underestimation in areas cultivated with rubber, rice, and cocoa, attributed to the scarcity of training data. In this regard, the findings of this research reaffirm the importance of a solid and representative field sampling design, capable of capturing the spectral and spatial variability of productive systems, to improve the quality of cartographic products in agricultural monitoring studies.

The main limitations faced in this research were the restricted access to high spatial resolution satellite imagery (<2 m), which generally requires payment. This constrained the analysis to images with resolutions of ≥10 m, limiting the detection of small patches. In addition, the frequent cloud cover in the study

area affected the availability of clean optical images, hindering the precise delineation of cultivated areas and other land cover types (Li et al. 2021). Similar situations have been reported by Kelley et al. (2018), when mapping complex shaded coffee landscapes in Nicaragua, where the integration of multiseasonal Landsat 8 images (30 m) in GEE yielded acceptable results, but were conditioned by the available spatial resolution. The intrinsic complexity of these agroforestry landscapes, with a heterogeneous mixture of trees and crops, also complicates classification tasks. Finally, the quality and quantity of field training data are fundamental; although more than 500 sampling points were collected in this study, obtaining representative information remains a challenge to ensure the reliability of the generated maps. To improve the mapping of shaded coffee in mountainous areas of Peru, it is recommended to combine satellite imagery with drones, or to use drones alone, to obtain more precise and detailed data in the future.

An additional challenge currently faced by export-oriented farmers is the implementation of new European regulations. Although this study shows an increase in coffee-growing areas, particularly from 2020 onward (Figure 8), this pattern cannot be directly attributed to the EUDR, as the regulation was published in June 2023 and its mandatory enforcement for operators and large companies is scheduled for late 2024–2025 (European Commission, 2023). Nevertheless, the results of the multitemporal analysis (2019–2024) reveal a sustained expansion and interannual stability in coffee cultivation. Considering the geospatial traceability requirements established by the EUDR, it is likely that production intended for regulated markets will remain stable or even increase within organised units such as cooperatives, whereas producers with lower levels of formalisation may face greater challenges in meeting compliance standards (Freitas Beyer et al. 2025). Consequently, under a scenario of progressive adaptation to the EUDR, it is reasonable to anticipate that the observed expansion trend will moderate, yet remain positive from 2026 onward.

5. Conclusions

This research demonstrates that the use of geospatial analysis platforms such as GEE, together with Sentinel–1 and Sentinel–2 satellite imagery, constitutes an effective tool for monitoring coffee-producing areas in Peru. The applied methodology enabled the identification of the spatial evolution of coffee cultivation with high precision between 2019 and 2024, showing a significant increase of 32.75% in cultivated area over six years (2,331.98 ha). These results not only help reduce existing information gaps regarding national coffee production, but also provide a reliable technical basis to support land-use planning, production traceability, and compliance with international regulations such as the EUDR. Finally, this approach is replicable and scalable for other crops and regions, thus promoting more sustainable and informed agricultural management aligned with global challenges such as climate change and deforestation.

Acknowledgements

The authors would like to thank the institutions 'Cooperativa Agraria Cafetalera Alta Montaña', 'Cooperativa Agraria y de Servicios Múltiples la Flor del Café de Rodríguez de Mendoza LTDA' and 'Cooperativa Agraria Rodriguez de Mendoza - COOPARM' for their support in the field work and data collection.

Author contributions

CRediT: **Angel J. Medina:** Conceptualization, Data curation, Formal analysis, Investigation, Methodology, Software, Validation, Visualization, Writing – original draft; **Rolando Salas López:** Conceptualization, Funding acquisition, Investigation, Methodology, Resources, Visualization; **Jhon A. Zabaleta-Santisteban:** Conceptualization, Investigation, Methodology, Validation, Writing – review & editing; **Katerin M. Tuesta-Trauco:** Formal analysis, Investigation, Methodology, Software, Validation; **Abner S. Rivera-Fernández:** Data curation, Investigation, Methodology, Validation; **José A. Sánchez-Vega:** Investigation, Methodology, Software, Validation; **Teodoro B. Silva-Melendez:** Investigation, Methodology, Visualization, Writing – review & editing; **Jhonsy O. Silva-López:** Investigation, Methodology; **Nilton B. Rojas Briceno:** Investigation, Methodology, Writing – review & editing; **Marlen A. Grandez Alberca:** Investigation, Methodology, Writing – review & editing; **Cecibel Portocarrero Díaz:** Investigation, Methodology, Project administration; **Jaris Veneros:** Investigation, Methodology, Writing – review & editing; **Manuel Oliva Cruz:** Funding acquisition, Investigation, Methodology; **Elgar Barboza:** Investigation, Methodology, Project administration, Resources, Supervision, Visualization, Writing – original draft.

Disclosure statement

No potential conflict of interest was reported by the author(s).

Funding

This work was subsidised by CONCYTEC through the PROCIENCIA programme under the 'Applied Research Projects 2024–01' competition, under contract PE501086161–2024-PROCIENCIA, and from the GEOMATICA public investment project (CUI N° 2255,626), executed by the Research Institute for Sustainable Development of Ceja de Selva (INDES-CES) of the Toribio Rodríguez de Mendoza National University in Amazonas. The APC was funded by the Vice-Rectorate for Research of the Universidad Nacional del Amazonas Toribio Rodríguez de Mendoza de Amazonas.

Data availability statement

The data used to support the findings of this study are available from the corresponding author upon request.

References

Adrian J, Sagan V, Maimaitijiang M. 2021. Sentinel SAR-optical fusion for crop type mapping using deep learning and google earth engine. ISPRS J Photogramm Remote Sens. 175(December 2020):215–235. https://doi.org/10.1016/j.isprsjprs.2021.02.018

Aji MAP, Kamal M, Farda NM. 2023. Mangrove species mapping through phenological analysis using random forest algorithm on google earth engine. Remote Sens Appl Soc Environ. 30:100978. https://doi.org/https://doi.org/10.1016/j.rsase.2023.100978

Atalaya-Marin N, et al. 2025. Integrating remote sensing and in-situ data to determine climate diversity and variability in cocoa systems in the provinces of Jaén and San Ignacio, Cajamarca (NW Perú). Trees, Forests and People. 19:100749. https://doi.org/https://doi.org/10.1016/j.tfp.2024.100749

Barboza E, et al. 2024. Spatial distribution of burned areas from 1986 to 2023 using cloud computing: a case study in Amazonas (Peru). Fire. 7(11):413. https://doi.org/10.3390/fire7110413

Becker WR, Ló TB, Johann JA, Mercante E. 2021. Statistical features for land use and land cover classification in google earth engine. Remote Sens Appl Soc Environ. 21:100459. https://doi.org/https://doi.org/10.1016/j.rsase.2020.100459

Bolívar S, Reu B. 2021. Detection and characterization of agroforestry systems in the Colombian Andes using sentinel-2 imagery. Agroforestry Systems. 95(3):499–514. https://doi.org/10.1007/s10457-021-00597-8

Breiman L. 2001. Random Forests. Mach Learn. 45(1):5–32. https://doi.org/10.1023/A:1010933404324

Campos Baca L, et al. 2019. Propuesta de zonificación ecológica y economica del departamento de Amazonas. Sustainability (Switzerland). 11(1):1–14. https://sinia.minam.gob.pe/sites/default/files/sinia/archivos/public/docs/estudio_de_la_propuesta_de_zee_0.pdf

Condro AA, Setiawan Y, Prasetyo LB, Pramulya R, Siahaan L. 2020. Retrieving the national main commodity maps in indonesia based on high-resolution remotely sensed data using cloud computing platform. Land. 9(10):1–15. https://doi.org/10.3390/land9100377

Cui J-T, Zhang X, Wang W-S, Wang L. 2020. Integration of optical and sar remote sensing images for crop-type mapping based on a novel object-oriented feature selection method. 13(1 PP-Beijing DT-International Journal of Agricultural and Biological Engineering), 178–190. https://doi.org/https://doi.org/10.25165/j.ijabe.20201301.5285

Dash J, Curran PJ. 2004. The MERIS terrestrial chlorophyll index. IJRS. 25(23):5403–5413. https://doi.org/10.1080/0143116042000274015

Escobar-López A, Castillo-Santiago MÁ, Hernández-Stefanoni JL, Mas JF, López-Martínez JO. 2022. Identifying coffee agroforestry system types using multitemporal sentinel-2 data and auxiliary information. Remote Sens. 14(16):1–15. https://doi.org/10.3390/rs14163847

Escobar-López A, Castillo-Santiago MA, Mas JF, Hernández-Stefanoni JL, López-Martínes JO. 2024. Identification of coffee agroforestry systems using remote sensing data: a review of methods and sensor data. Geocarto Int. 39(1), https://doi.org/10.1080/10106049.2023.2297555

European Commission. 2023. EU Regulation on deforestation-free products (EUDR). Official Journal of the European Union.

European Commission. 2024. Reglamento sobre productos libres de deforestación - Comisión Europea. https://environment.ec.europa.eu/topics/forests/deforestation/regulation-deforestation-free-products_en

European Parliament. 2022. The documents that help shape new EU legislation. https://www.europarl.europa.eu/thinktank/en/home

Fangjie L, Shabarinath N, Inbal BR, Françoise N. 2023. Integrating multiple remote sensing data for coffee mapping in Kenya. Transition Resources. 2023(21):B21E-2008. https://ui.adsabs.harvard.edu/abs/2023AGUFM.B21E2008L/abstract
FAOSTAT. 2024. Food and Agriculture Organization of the United Nations. https://www.fao.org/FAOSTAT/en/#data/QCL/visualize
Farr TG et al. 2007. The shuttle radar topography mission. Reviews of Geophys. 45(2). https://doi.org/10.1029/2005RG000183
Ferreira CO, Grego CR, Manzione RL, Madeiros SR. 2024. Improving coffee yield interpolation in the presence of outliers using multivariate geostatistics and satellite data. AgriEngineering. 6(1):81–94. https://doi.org/10.3390/agriengineering6010006
Freitas Beyer J, Köthke M, Lippe M. 2025. Assessing the suitability of available global forest maps as reference tools for EUDR-compliant deforestation monitoring. Remote Sens. 17(17):1–28. https://doi.org/10.3390/rs17173012
Gao B. 1996. NDWI—A normalized difference water index for remote sensing of vegetation liquid water from space. Remote Sens Environ. 58(3):257–266. https://doi.org/https://doi.org/10.1016/S0034-4257(96)00067-3
García MJL, Caselles V. 1991. Mapping burns and natural reforestation using thematic mapper data. GeoIn. 6(1):31–37. https://doi.org/10.1080/10106049109354290
García L, Veneros J, Oliva-Cruz M, Olivares N, Chavez SG, Rojas-Briceño NB. 2024. Construction of linear models for the normalized vegetation index (NDVI) for coffee crops in Peru based on historical atmospheric variables from the climate engine platform. Atmosphere. 15(8):923. https://doi.org/10.3390/atmos15080923
Gitelson AA, Vina A, Arkebauer TJ, Rundquist DC, Keydan G, Leavitt B. 2003. Remote estimation of leaf area index and green leaf biomass in maize canopies. Geophys Res Lett. 30(5):4–7. https://doi.org/10.1029/2002gl016450
Gómez Fernández D, Salas López R, Rojas Briceño NB, Silva López JO, Oliva M. 2022. Dynamics of the burlan and Pomacochas lakes using SAR data in GEE, machine learning classifiers, and regression methods. IJGI. 11(11):534. https://doi.org/10.3390/ijgi11110534
Gómez-Fernández D, et al. 2024. Landsat images and GIS techniques as key tools for historical analysis of landscape change and fragmentation. Ecological Informatics. 82:102738. https://doi.org/https://doi.org/10.1016/j.ecoinf.2024.102738
Google Earth Engine. 2025. Algoritmos de Sentinel-1 | Google Earth Engine | Google para desarrolladores. https://developers.google.com/earth-engine/guides/sentinel1?hl=es-419
Grandez-Alberca MA, et al. 2025. Agronomic and economic sustainability perspectives in coffee-based agroforestry system (Coffea arabica L.) in Rodríguez de Mendoza, Amazonas, Peru. Trees, Forests and People. 21:100924. https://doi.org/https://doi.org/10.1016/j.tfp.2025.100924
Gumma MK, Thenkabail PS, Panjala P, Teluguntla P, Yamano T, Mohammed I. 2022. Multiple agricultural cropland products of South Asia developed using Landsat-8 30 m and MODIS 250 m data using machine learning on the google earth engine (GEE) cloud and spectral matching techniques (SMTs) in support of food and water security. GIScience and Remote Sensing. 59(1):1048–1077. https://doi.org/10.1080/15481603.2022.2088651
Harmonized Sentinel-2 MSI: MultiSpectral Instrument, Level-2A (SR) | Earth Engine Data Catalog | Google for Developers. (n.d.). Retrieved August 18, 2025, from https://developers.google.com/earth-engine/datasets/catalog/COPERNICUS_S2_SR_HARMONIZED?hl=es-419#bands
Hobbs PR, Sayre K, Gupta R. 2007. The role of conservation agriculture in sustainable agriculture. Philos Trans R Soc Lond B Biol Sci. 363(1491):543–555. https://doi.org/10.1098/RSTB.2007.2169
Houghton RA, Lawrence KT, Hackler JL, Brown S. 2001. The spatial distribution of forest biomass in the brazilian Amazon: a comparison of estimates. Global Change Biol. 7(7):731–746. https://doi.org/10.1111/J.1365-2486.2001.00426.X
Htitiou A, Boudhar A, Chehbouni A, Benabdelouahab T. 2021. National-scale cropland mapping based on phenological metrics, environmental covariates, and machine learning on google earth engine. Remote Sens. 13(21):1–26. https://doi.org/10.3390/rs13214378
Huete A, Didan K, Miura T, Rodriguez EP, Gao X, Ferreira LG. 2002. Overview of the radiometric and biophysical performance of the MODIS vegetation indices. Remote Sens Environ. 83(1):195–213. https://doi.org/https://doi.org/10.1016/S0034-4257(02)00096-2
Hunt DA et al. 2020. Review of Remote Sensing Methods to Map Coffee Production Systems. Remote Sens. 12(12):1–23. https://doi.org/https://doi.org/10.3390/rs12122041
ICO. 2024. International Coffee Organization. https://icocoffee.org/
INEI. 2017. Perú: Estimaciones y Proyecciones de Población por Departamento, Provincia y Distrito, 2018–2020. Inei, 1–110. https://www.inei.gob.pe/media/MenuRecursivo/publicaciones_digitales/Est/Lib1715/libro.pdf
Kelley LC, Pitcher L, Bacon C. 2018. Using google earth engine to map complex shade-grown coffee landscapes in Northern Nicaragua. Remote Sens. 10(6). https://doi.org/10.3390/rs10060952. .
Landis JR, Koch GG. 1977. The Measurement of observer agreement for categorical data. Biometrics. 33(1):159. https://doi.org/10.2307/2529310
Li Y, Liu C, Zhang J, Zhang P, Xue Y. 2021. Monitoring spatial and temporal patterns of rubber plantation dynamics using time-series landsat images and google earth engine. IJSTA. 14:9450–9461. https://doi.org/10.1109/JSTARS.2021.3110763
Liu X, Frey J, Munteanu C, Still N, Koch B. 2023. Mapping tree species diversity in temperate montane forests using Sentinel-1 and Sentinel-2 imagery and topography data. Remote Sens Environ. 292(March):113576. https://doi.org/10.1016/j.rse.2023.113576

Maskell G, Chemura A, Nguyen H, Gornott C, Mondal P. 2021a. Integration of Sentinel optical and radar data for mapping smallholder coffee production systems in Vietnam. Remote Sens Environ. 266(February):112709. https://doi.org/10.1016/j.rse.2021.112709
Maskell G, Chemura A, Nguyen H, Gornott C, Mondal P. 2021b. Integration of Sentinel optical and radar data for mapping smallholder coffee production systems in Vietnam. Remote Sens Environ. 266:112709. https://doi.org/https://doi.org/10.1016/j.rse.2021.112709
Medina-Medina AJ, et al. 2024. An analysis of the rice-cultivation dynamics in the lower Utcubamba river basin using SAR and optical imagery in google earth engine (GEE). Agronomy. 14(3):557. https://doi.org/10.3390/agronomy14030557
Moguel P, Toledo VM. 1999. Biodiversity conservation in traditional coffee systems of Mexico. Conserv Biol. 13(1):11–21. https://doi.org/10.1046/j.1523-1739.1999.97153.x
Moraiti N, Mullissa A, Rahn E, Sassen M, Reiche J. 2024. Critical assessment of cocoa classification with limited reference data: a study in Côte d'Ivoire and Ghana Using Sentinel-2 and random forest model. Remote Sens. 16(3):598. https://doi.org/10.3390/rs16030598
Nadaf SA, et al. 2024 Coffee (Coffea spp.) BT - Soil Health Management for Plantation Crops: Recent Advances and New Paradigms (G. V. Thomas & V. Krishnakumar (Eds.); pp. 337–389). Springer Nature Singapore. https://doi.org/10.1007/978-981-97-0092-9_9
Onojeghuo AO, Miao Y, Blackburn GA. 2023. Deep ResU-net convolutional neural networks segmentation for smallholder paddy rice mapping using sentinel 1 SAR and sentinel 2 optical imagery. Remote Sens. 15(6):1–20. https://doi.org/10.3390/rs15061517
Ouma Y, et al. 2022. Comparison of machine learning classifiers for multitemporal and multisensor mapping of urban lulc features. International Archives of the Photogrammetry, Remote Sensing and Spatial Information Sciences - ISPRS Archives. 43(B3-2022):681–689. https://doi.org/10.5194/ISPRS-ARCHIVES-XLIII-B3-2022-681-2022
Pahlevan N, et al. 2020. ACIX-Aqua: A global assessment of atmospheric correction methods for Landsat-8 and Sentinel-2 over lakes, rivers, and coastal waters. Remote Sens Environ. 258:2021. https://doi.org/10.1016/j.rse.2021.112366
Qi J, Chehbouni A, Huete AR, Kerr YH, Sorooshian S. 1994. A modified soil adjusted vegetation index. Remote Sens Environ. 48(2):119–126. https://doi.org/https://doi.org/10.1016/0034-4257(94)90134-1
Rojas-Briceño NB, et al. 2025. Effectiveness of protected areas in containing the loss of Peruvian Amazonian forests. Trees, Forests and People. 19:100778. https://doi.org/https://doi.org/10.1016/j.tfp.2025.100778
Rouse JW, Haas RH, Schell JA, Deering DW. 1973. Monitoring the vernal advancement and retrogradation (green wave effect) of natural vegetation. Progress Report RSC. 1. https://ntrs.nasa.gov/api/citations/19730017588/downloads/19730017588.pdf
Salas R, et al. 2020. Land suitability for coffee (coffea arabica) growing in Amazonas, Peru: integrated use of AHP, GIS and RS. IJGI. 9(11):1–21. https://doi.org/10.3390/ijgi9110673
Sarzynski T, Giam X, Carrasco L, Huay Lee JS. 2020. Combining radar and optical imagery to map oil palm plantations in Sumatra, Indonesia, using the google earth engine. Remote Sens. 12(7):1220. https://doi.org/10.3390/rs12071220
Shelestov A, Lavreniuk M, Kussul N, Novikov A, Skakun S. 2017. Exploring google earth engine platform for big data processing: classification of multi-temporal satellite imagery for crop mapping. FrEaS. 5(February):1–10. https://doi.org/10.3389/feart.2017.00017
Single-Page API Reference | Google Earth Engine | Google for Developers. (n.d.). Retrieved July 19, 2024, from https://developers.google.com/earth-engine/api_docs
Thenkabail PS, Smith RB, De Pauw E. 2000. Hyperspectral vegetation indices and their relationships with agricultural crop characteristics. Remote Sens Environ. 71(2):158–182. https://doi.org/https://doi.org/10.1016/S0034-4257(99)00067-X
dela Torre DMG, Gao J, Macinnis-Ng C, Shi Y. 2021. Phenology-based delineation of irrigated and rain-fed paddy fields with Sentinel-2 imagery in google earth engine. Geo-Spatial Information Science. 24(4):695–710. https://doi.org/10.1080/10095020.2021.1984183;CTYPE:STRING:JOURNAL
van Beijma S, Comber A, Lamb A. 2014. Random forest classification of salt marsh vegetation habitats using quad-polarimetric airborne SAR, elevation and optical RS data. Remote Sens Environ. 149:118–129. https://doi.org/https://doi.org/10.1016/j.rse.2014.04.010
Van Deventer AP, Ward AD, Gowda PM, Lyon JG. 1997. Using thematic mapper data to identify contrasting soil plains and tillage practices. PgERS. 63(1):87–93.
Vilela EF, et al. 2023. New spectral index and machine learning models for detecting coffee leaf miner infestation using sentinel-2 multispectral imagery. Agriculture (Switzerland). 13(2):388. https://doi.org/10.3390/agriculture13020388
Vilela EF, et al. 2024. Remote monitoring of coffee leaf miner infestation using machine learning. AgriEngineering. 6(2):1697–1711. https://doi.org/10.3390/agriengineering6020098
Vincent MJ, Varalakshmi P. 2024. Agroforestry mapping using multi temporal hybrid CNN+LSTM framework with landsat 8 satellite imagery and google earth engine. Environ res commun. 6. https://doi.org/10.1088/2515-7620/ad549f
Vincent M J, Varalakshmi P. 2024. Agroforestry mapping using multi temporal hybrid CNN+LSTM framework with landsat 8 satellite imagery and google earth engine. ERCom. 6(6):065009. https://doi.org/10.1088/2515-7620/ad549f
Wang X, Fang S, Yang Y, Du J, Wu H. 2023. A new method for crop type mapping at the regional scale using multi-source and multi-temporal sentinel imagery. Remote Sens. 15. https://doi.org/https://doi.org/10.3390/rs15092466

Wyss O. 2015. Sentinel-2 User Handbook. Ind Eng Chem. 48(9):64. https://doi.org/10.1021/ie51400a018
Xu H. 2006. Modification of normalised difference water index (NDWI) to enhance open water features in remotely sensed imagery. IJRS. 27(14):3025–3033. https://doi.org/10.1080/01431160600589179
Yang L, Driscol J, Sarigai S, Wu Q, Chen H, Lippitt CD. 2022. Google earth engine and artificial intelligence (AI): a comprehensive review. Remote Sens. 14(14):3253. https://doi.org/10.3390/rs14143253
Zeng J et al. 2022. Optimization of open-access optical and radar satellite data in google earth engine for oil palm mapping in the Muda river basin, Malaysia. Agriculture. 12(9). https://doi.org/10.3390/agriculture12091435
Zhi F, et al. 2022. Rapid and automated mapping of crop type in Jilin province using historical crop labels and the google earth engine. Remote Sens. 14(16):1–19. https://doi.org/10.3390/rs14164028